RESEARCH ARTICLE

Allometry in desert ant locomotion (*Cataglyphis albicans* and *Cataglyphis bicolor*) – does body size matter?

Johanna Tross*, Harald Wolf* and Sarah Elisabeth Pfeffer*

ABSTRACT

Desert ants show a large range of adaptations to their habitats. They can reach extremely high running speeds, for example, to shorten heat stress during foraging trips. It has recently been examined how fast walking speeds are achieved in different desert ant species. It is intriguing in this context that some species exhibit distinct intraspecific size differences. We therefore performed a complete locomotion analysis over the entire size spectrum of the species *Cataglyphis bicolor*, and we compared this intraspecific dataset with that of the allometrically similar species *Cataglyphis albicans*. Emphasis was on the allometry of locomotion: we considered the body size of each animal and analysed the data in terms of relative walking speed. Body size was observed to affect walking parameters, gait patterns and phase relationships in terms of absolute walking speed. Unexpectedly, on a relative scale, all ants tended to show the same overall locomotion strategy at low walking speeds, and significant differences occurred only between *C. albicans* and *C. bicolor* at high walking speeds. Our analysis revealed that *C. bicolor* ants use the same overall strategy across all body sizes, with small ants reaching the highest walking speeds (up to 80 body lengths s^{-1}) by increasing their stride length and incorporating aerial phases. By comparison, *C. albicans* reached high walking speeds mainly by a high synchrony of leg movement, lower swing phase duration and higher stride frequency ranging up to 40 Hz.

KEY WORDS: Desert ant, Insect model, Locomotion strategy, Walking speed, Aerial phases

INTRODUCTION

Locomotion of ants, and more generally of insects, has fascinated scientists for decades (e.g. Hughes, 1952; Wilson, 1966). In recent years, walking behaviour and locomotion studies have yielded important insights, many of them rendered possible by the latest advanced methods. Together with several other insect model systems, such as stick insects and cockroaches (Ayali et al., 2015; Dürr et al., 2018), ants have become well-studied subjects in insect locomotion, providing a source for current biomechanical and neuroethological findings. Recent studies tackle the problem of locomotion on inclines and uneven substrates (Humeau et al., 2019; Clifton et al., 2020) or implement insect data into bio-inspired legged robots (Yeoh and Yi, 2021). In the case of *Cataglyphis* desert ants, many aspects have been studied in detail, including strategies

to reach high walking speeds (Zollikofer, 1994a; Wahl et al., 2015; Pfeffer et al., 2019), walking behaviour on inclines (Seidl and Wehner, 2008), the influence of temperature (Hurlbert et al., 2008), body morphology (Hurlbert et al., 2008; Zollikofer, 1994b) and load changes (Zollikofer, 1994c), or navigation performance during backward and forward walking (Pfeffer et al., 2016). However, a complete locomotion analysis over a broad walking speed range including the influence of body size has never been performed in this context. Few studies on ants (Burd, 2000; Hurlbert et al., 2008) and also spiders (Prenter et al., 2010, 2012) investigated the influence of body size on locomotion but walking speed was often used as main measure of locomotion.

Cataglyphis desert ants are able to occupy an ecological niche that is lethal to many other animals. They forage during the hottest hours of the day, and times of the year, without succumbing to heat stress, while most other insects and animal groups retreat to cooler refuges during much of the day (Wehner, 1983; Wehner and Wehner, 2011). To withstand the extreme conditions of the desert, *Cataglyphis* ants have evolved outstanding physiological (Gehring and Wehner, 1995), morphological (Sommer and Wehner, 2012) and behavioural adaptions (Wehner and Wehner, 2011). A positive correlation between leg length and habitat temperature has been observed in this context (Sommer and Wehner, 2012). Long legs allow high walking speeds, increasing air convection and thus cooling the body during the run. Above all, fast and energy-efficient locomotion is essential to shorten heat stress during foraging trips and dwell in nutritionally sparse desert habitats (Wahl et al., 2015; Pfeffer et al., 2019).

The genus *Cataglyphis* includes about 100 species with considerable variation in body size (Agosti, 1990). Within the genus, *C. bicolor* (Fabricius, 1793) is among the largest species. Mesosoma lengths of *C. bicolor* range from 2.1 to 5.0 mm, demonstrating a striking spectrum in body size, with the distribution skewed toward larger individuals (Sommer and Wehner, 2012). One of the smallest *Cataglyphis* ant species is *C. albicans* (Roger, 1859), exhibiting comparatively little variation in mesosoma length (1.6 to 2.7 mm) with up to 3.2 mm reported previously (Agosti, 1990; Sommer and Wehner, 2012). Regarding body size, the two species overlap; that is, the largest *C. albicans* exceed the size of the smallest *C. bicolor* individuals. The influence of body size on locomotion over a broad speed range has rarely been investigated, either among ant species or in insects in general. These two *Cataglyphis* species thus offer themselves for such investigation. One may assume that differences in body size and associated leg length affect locomotion. Significant differences in body size should influence walking behaviour of individuals within a given species, as well as in a comparison between species.

In the present study, we analysed the locomotion of desert ants along gradients in both body size and walking speed, using *C. bicolor* and *C. albicans* as two species whose body sizes merge seamlessly into each other (Fig. 1, Fig. 2). Body size was taken as a
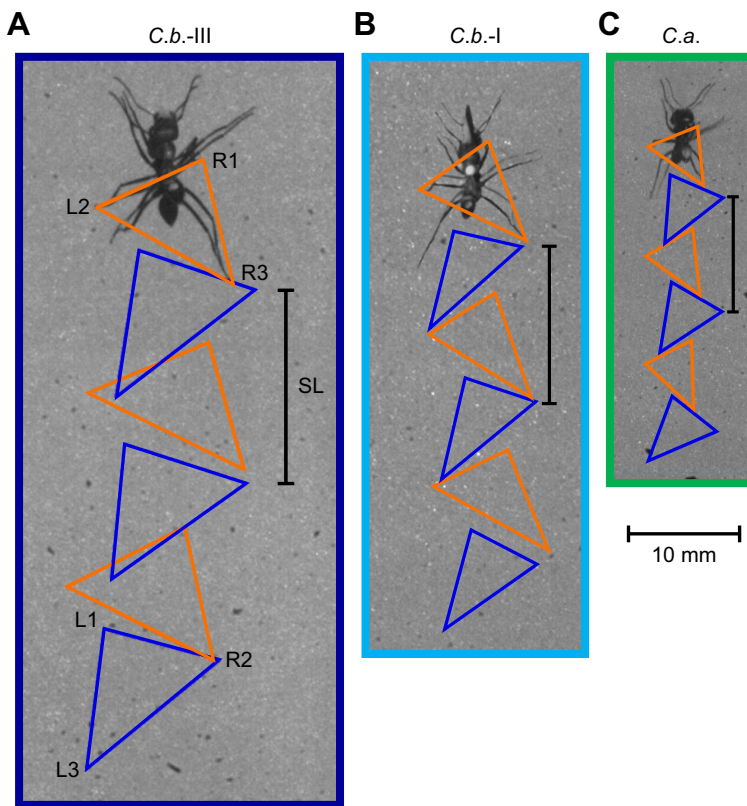
Fig. 1. Tripod gait in *Cataglyphis bicolor* and *Cataglyphis albicans*. Frame from a high-speed video showing an ant from the *C. bicolor* large (A) and small (B) groups and from the *C. albicans* group (C) at the same absolute walking speeds. For each leg, three consecutive step cycles were recorded in the corresponding video frames (sampling rate 900 Hz). Tripods of the left front (L1), hind (L3) and right middle (R2) legs are indicated by blue triangles; opposite tripods (R1, L2, R3) are indicated by orange triangles. Stride length (SL) is indicated for the right middle leg. (A) *C.b.*-III: mesosoma length ML=4.16 mm, velocity v=376 mm s^{-1}, SL=17.5 mm; the ant has a small food item in its mandibles; (B) *C.b.*-I: ML=2.95 mm, v=367 mm s^{-1}, SL=13.9 mm; the ant has a long food item in its mandibles; (C) *C.a.*: ML=2.06 mm, v=374 mm s^{-1}, SL=10 mm.

reference to analyse all parameters with regard to relative walking speed (mesosoma lengths per second). The allometry of locomotion was considered in an intraspecific as well as interspecific comparison.

MATERIALS AND METHODS
Ant colonies and experimental conditions
Ants of the species *Cataglyphis bicolor* (Fabricius 1793) and *Cataglyphis albicans* (Roger 1859) were obtained from colonies in their natural habitats near Mahrés, Tunisia (34.53°N, 10.49°S). To analyse the walking parameters in small (*C.b.*-I, 2.4–3.5 mm), medium-sized (*C.b.*–II, 3.5–4.0 mm) and large *C. bicolor* individuals (*C.b.*-III, 4.0–5.0 mm) and in *C. albicans* (*C.a.*, 1.5–2.7 mm) ants, high-speed videos were recorded in the field near Mahrés, and under laboratory conditions at Ulm University, Germany (48.42°N, 9.95°S). For recordings in the laboratory, ants of both species were kept under constant temperature (28°C) and daily light:dark cycles (14 h:10 h), roughly corresponding to their natural habitat conditions. Note that the two datasets merge smoothly regarding all observed parameters (no notable changes in walking parameter trend lines), even though temperatures and walking speeds tend to be higher in the desert than in Germany.

All data [*C.a.* n=60 runs (at different temperatures as for the following groups), n=12 ants; *C.b.*–I n=57 runs, n=19 ants; *C.b.*-II n=47 runs, n=20 ants; and *C.b.*-III n=74 runs, n=28 ants] were obtained during 2016 and 2018. The experiments were conducted in compliance with the current laws and ethical guidelines of Ulm University and the countries where they were performed.

Data for *C.b.*–II (medium-sized ants of *C. bicolor*) were also analysed but not included for clarity of illustration. The range of medium-sized ants is smaller than that of both *C.b.*-I and *C.b.*–III, and was chosen to clearly delineate the small and large individuals and avoid blurring of relevant differences. All data for *C.b.*-II are
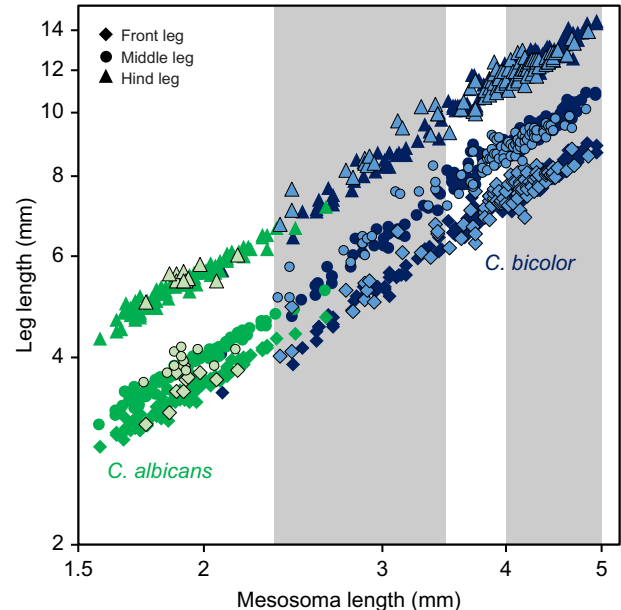

Fig. 2. Morphometric analysis. Correlation between mesosoma length and leg length in *C. albicans* (n=109, green) and *C. bicolor* (n=240, blue). Data for the front legs (power function: *C. albicans*: $y=1.88x^{0.95}$, R^2=0.94; *C. bicolor*: $y=1.64x^{1.07}$, R^2=0.96), middle legs (power function: *C. albicans*: $y=2.11x^{0.93}$, R^2=0.94; *C. bicolor*: $y=1.90x^{1.09}$, R^2=0.96) and hind legs (power function: *C. albicans*: $y=3.01x^{0.88}$, R^2=0.94; *C. bicolor*: $y=2.75x^{1.02}$, R^2=0.96) are plotted separately. Data for ants used for high-speed analysis are indicated in light colours with black outlines. Further, the ranges of small (*C.b.*-I, ML: 2.5–3.5 mm) and large (*C.b.*-III, ML: 4–5 mm) *C. bicolor* are marked in grey. Detailed allometric comparison is given in Tables S1 and S2.

intermediate between those of *C.b.*-I and *C.b.*-III in both morphometry and locomotion.

Morphometric analysis

For morphometric comparison, the length of the mesosoma (i.e. alitrunk, fused thorax and first abdominal segment) and the three leg pairs was determined in *C. bicolor* and *C. albicans* ants that we used for high-speed analysis. All measurements were performed under a dissection microscope (Stemi SV 6, Zeiss Microscopy GmbH, Jena, Germany), and photos were taken with a camera and calibration eyepiece. The images were evaluated with ImageJ (National Institutes of Health, Bethesda, MD, USA). Before measurements, the gaster was removed and the six legs were severed at the coxa–thorax joints. The length of the femur, tibia and basitarsus was determined for the front, middle and hind legs. The respective values of the femur, tibia and basitarsus of the left and right front, middle and hind legs were added, and means for the three leg pairs were calculated. Mesosoma length was used to characterize body size (see fig. 8 in Andersen et al., 2020) and was the main characteristic to subdivide *C. bicolor* ants into three different size classes.

To describe the relationship between mesosoma length and leg length within and between species, we used the allometric equation $y=a\times x^{b}$. Scaling factor a and exponent b were estimated for ants of both species (see also Sommer and Wehner, 2012). To supplement the morphometric data, we were kindly allowed to use the data from Sommer and Wehner (2012) (*C. bicolor*: $n=142$ and *C. albicans*: $n=97$). Thus, a total of 240 ants of *C. bicolor* and 109 ants of *C. albicans* were used for the morphometric analysis.

High-speed videos and experimental procedures

High-speed video recordings were made with a high-speed camera (MotionBlitz EoSense Mini1, Mikrotron Unterschleissheim, Germany; Nikon Lens 105 mm 1:2.8 DG MACRO, Japan) at 900, 910 and 999 frames s^{-1} in Tunisia and at 500 and 711 frames s^{-1} under laboratory conditions in Ulm, Germany. Different frame rates were used because of walking speed differences and for maximum pixel size reasons. Example videos are available in the supplementary information (Movies 1 and 2).

The ants were filmed while walking through a linear aluminium channel with a width of 7 cm and a wall height of 7 cm. For recordings, the camera was mounted above the channel to provide a top view of the ants. The channel floors were coated with a layer of fine white sand (0.1–0.4 mm particle size) to provide a slip-free floor for normal walking behaviour. To avoid reflections, the channel walls were painted with matt grey varnish. The highest walking speeds were usually recorded in Mahrés, Tunisia, around noon (11:00 h to 15:00 h), when the highest air temperatures (~45°C) were reached at the field site. Under laboratory conditions in Ulm, Germany, the channel was lined with white print paper below the camera to reduce reflections and provide better contrast. Ants were filmed at different controlled room temperatures (10–45°C) to obtain the complete walking speed range. For indoor illumination, two fibre optic cold light sources (Schott KL 1500LCD, 150 W, Schott AG, Mainz, Germany) were used.

The ants were usually filmed several (up to 5) times at different temperatures to obtain different walking speeds. Only straight and smooth running trajectories were used for the analysis. Walking sequences with stops, decelerations, curves and slipping steps were disregarded. Furthermore, each evaluated high-speed video had to consist of a minimum of three complete step cycles per leg. For calibration, a piece of millimetre grid paper was used.

All measurements were analysed in a frame-by-frame video analysis with ImageJ (National Institutes of Health).

Analysis of high-speed videos and data analysis
Walking parameters

To analyse and compare walking patterns in small, medium and large *C. bicolor* individuals and in *C. albicans* ants, different walking parameters were analysed (Fig. 3). Mean walking speed was calculated as the distance covered from the beginning of the first to the end of the third step cycle, divided by the time the ants needed to cover this distance. We only analysed videos with a constant mean walking speed over the three step cycles. Relative walking speed was defined as mean walking speed divided by mesosoma length. Further, the timing of every lift-off and touch-down of the six legs was measured to obtain swing phase and stance phase durations. These values formed the basis for all further evaluations of walking parameters and for gait analysis. Swing phase duration was calculated as the time difference between tarsal lift-off and touch-down. Stance phase duration was defined as the period of time over which the tarsal tip touched and did not move relative to the ground (Reinhardt and Blickhan, 2014; Wahl et al., 2015). Stride length was calculated as the distance between tarsal lift-off and touch-down positions for the respective leg pair. To determine stride frequency, we divided mean walking speed by stride length. Swing speed (allocentric coordinates) was defined as stride length divided by the respective swing phase duration for the respective leg pairs. All parameters described above were averaged for all six legs, as no notable differences were observed between the respective legs (see Fig. S1, single leg pair analysis).

Footfall geometry

In a frame-by-frame analysis, the x and y coordinates of tarsal lift-off (posterior extreme position, PEP) and tarsal touch-down (anterior extreme position, AEP) were measured for each leg with respect to the centre of mass (COM, assumed to reside in the petiole; Reinhardt and Blickhan, 2014) to quantify footfall geometry (see also Seidl and Wehner, 2008; Mendes et al., 2013; Pfeffer et al., 2019). Footfall positions relative to the COM were normalized to mesosoma length, and standard deviations of the resulting values were used to illustrate the spread of footfall positions (Fig. 4). To track the movements of the legs and to analyse footfall geometry, we used ImageJ (National Institutes of Health), Excel (Microsoft Corporation, Redmond, WA, USA) and Sigma Plot 11.0 (Systat Software Inc., San Jose, CA, USA).

Phase analysis

To evaluate the synchrony of tripod coordination, we calculated tripod coordination strength (TCS) (Wosnitza et al., 2013). We determined t_1, as the time period with all three legs of a tripod group concurrently in swing phase, and t_2 as the time period from the first swing onset in any of the legs in the tripod to the last swing termination. t_2 thus indicates the period where at least one of the three legs of the tripod group is in swing phase. The ratio t_1/t_2 is taken as the TCS value. A TCS value of 1.0 indicates perfect tripod coordination, and a value approaching 0 indicates that leg movements have assumed other coordination patterns (Wosnitza et al., 2013).

For phase analyses, the beginning of the swing phase in the left hind leg was taken as a reference (Fig. 5). Phase plots show the coordination of the six legs in a circular step cycle diagram. They were created with the 'CircStat' Toolbox in MATLAB (MathWorks, Inc., Natick, MA, USA) (Berens, 2009). Furthermore, we calculated

Absolute walking parameters

Relative walking parameters

Fig. 3. See next page for legend.

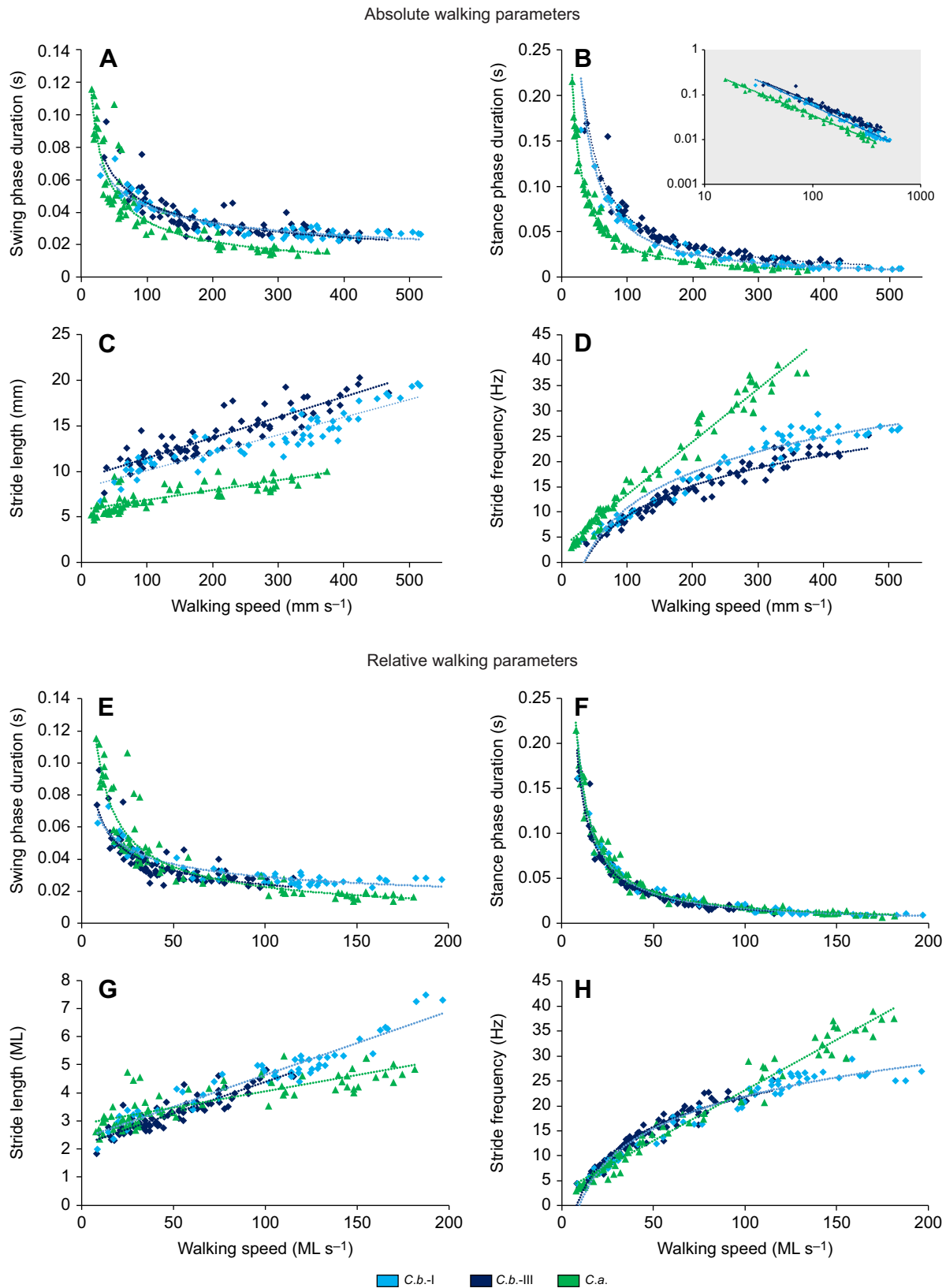duty factor as the ratio of stance phase to cycle period (stance plus swing phase of a given stride). Duty factor characterizes the transition from walking to running. Considering a particular pair of legs, a duty factor value of 0.5 signifies the point where aerial phases have to be integrated into the gait pattern to achieve higher speeds (Alexander, 2003). In animals walking on more than one leg

Fig. 3. Walking parameters. The most significant walking parameters in *C. albicans* and *C. bicolor* plotted as functions of absolute (mm s^{-1}) and relative walking speed (ML s^{-1}). Each data point represents the mean value of the three leg pairs in a video sequence (*C.b.*-I: $n=57$, light blue; *C.b.*–III: $n=75$, dark blue; *C.a.*: $n=73$, green). (A–D) Absolute walking parameters: (A) swing phase duration (power functions: *C.b.*-I: $y=0.25x^{-0.38}$, $R^2=0.85$; *C.b.*-III: $y=0.35x^{-0.44}$, $R^2=0.73$; *C.a.*: $y=0.66x^{-0.64}$, $R^2=0.91$); (B) stance phase duration (power functions: *C.b.*-I: $y=9.55x^{-1.12}$, $R^2=0.97$; *C.b.*-III: $y=6.84x^{-1.00}$, $R^2=0.96$; *C.a.*: $y=3.50x^{-1.00}$, $R^2=0.98$); inset: log–log plot of stance phase duration; (C) stride length (linear regressions: *C.b.*-I: $y=0.02x+8.18$, $R^2=0.84$; *C.b.*–III: $y=0.02x+9.23$, $R^2=0.79$; *C.a.*: $y=0.01x+5.75$, $R^2=0.64$); (D) stride frequency (logarithmic regressions: *C.b.*–I: $y=10.16\ln x−36.02$, $R^2=0.93$; *C.b.*-III: $y=8.67\ln x−30.75$, $R^2=0.92$; linear regression: *C.a.*: $0.11x+2.85$, $R^2=0.97$). (E–H) Relative walking parameters: (E) swing phase duration (power functions: *C.b.*-I: $y=0.14x^{-0.35}$, $R^2=0.86$; *C.b.*-III: $y=0.18x^{-0.44}$, $R^2=0.72$; *C.a.*: $y=0.42x^{-0.64}$, $R^2=0.91$); (F) stance phase duration (power functions: *C.b.*-I: $y=1.84x^{-1.02}$, $R^2=0.97$; *C.b.*-III: $y=1.61x^{-1.01}$, $R^2=0.97$; *C.a.*: $y=1.72x^{-0.993}$, $R^2=0.98$); (G) relative stride length (linear regressions: *C.b.*-I: $y=0.05x+8.88$, $R^2=0.73$; *C.b.*-III: $y=0.09x+9.34$, $R^2=0.77$; *C.a.*: $y=0.02x+5.75$, $R^2=0.63$); (H) stride frequency (logarithmic regressions: *C.b.*-I: $y=9.36\ln x−21.19$, $R^2=0.95$; *C.b.*-III: $y=8.70\ln x−18.22$, $R^2=0.93$; linear regression: *C.a.*: $y=0.20x+2.89$, $R^2=0.97$).

pair, phase shifts between the leg pairs can still avoid aerial phases for the whole animal (Hildebrand, 1985). Nonetheless, duty factor remains a valuable parameter to address the potential presence of aerial phases, in particular when considering all leg pairs.

Gait analysis
Gait patterns were assessed using a frame-by-frame video analysis. Sequences of swing and stance movements of the six legs were visualized by podograms (qualitative gait analysis; Fig. 6). Podograms illustrate the gait patterns of the six legs with black bars indicating swing phases and white bars indicating stance phases. Further, we quantified the inter-leg coordination by classifying each frame according to its momentary gait pattern (see Mendes et al., 2013; Pfeffer et al., 2019). Inter-leg coordination data were compared quantitatively for different walking speed

ranges in the *C. bicolor* size groups, *C.b.*-I and *C.b.*–III, and in *C. albicans* (Fig. 7; Fig. S4). To this end, an index number and a respective index colour were assigned to each frame, corresponding to the momentary leg coordination. The index colour was used for illustration and the index number for statistical analysis. We defined the following gait categories, stance phase (−1, brown), pentapod (1, purple), tetrapod (2, lilac), tripod (3, dark green), bipod (4, yellow), monopod (5, orange) and aerial phase (6, red). Other leg coordinations were classified as undefined (0, grey). For a more detailed description, see Figs 6 and 7, and regarding particular gait categories, Fig. S3. To calculate a gait pattern index, we used MATLAB environment (MathWorks, Inc.).

Statistical analysis
Normality tests, statistical pairwise and multiple comparisons and box-and-whisker plots were generated in SigmaPlot 11.0 (Systat Software Inc.). The box-and-whisker plots show the median as the centre of the box, the 25th and the 75th percentiles as box margins and the 90th percentiles as whiskers. To scrutinize normal data distributions, the Shapiro–Wilk test was used. For multiple comparisons of normally distributed data, we used a one-way ANOVA with Holm–Šidák's method as *post hoc* test, and for non-normally distributed data, we used an ANOVA on ranks with Dunn's method as *post hoc* test. For comparison of circular data, we employed the MATLAB 'CircStat' Toolbox (Berens, 2009). Significance levels are indicated by asterisks in the figures. Final editing of the figures and tables was performed in Inkscape (Inkscape 1.0).

RESULTS
The allometry of locomotion was analysed for intraspecific and interspecific comparison. We examined differences in walking behaviour between small (*C.b.*-I) and large (*C.b.*-III) *C. bicolor* individuals and compared these data to those of the even smaller ants of the species *C. albicans* (*C.a.*) (Fig. 1). All parameters were
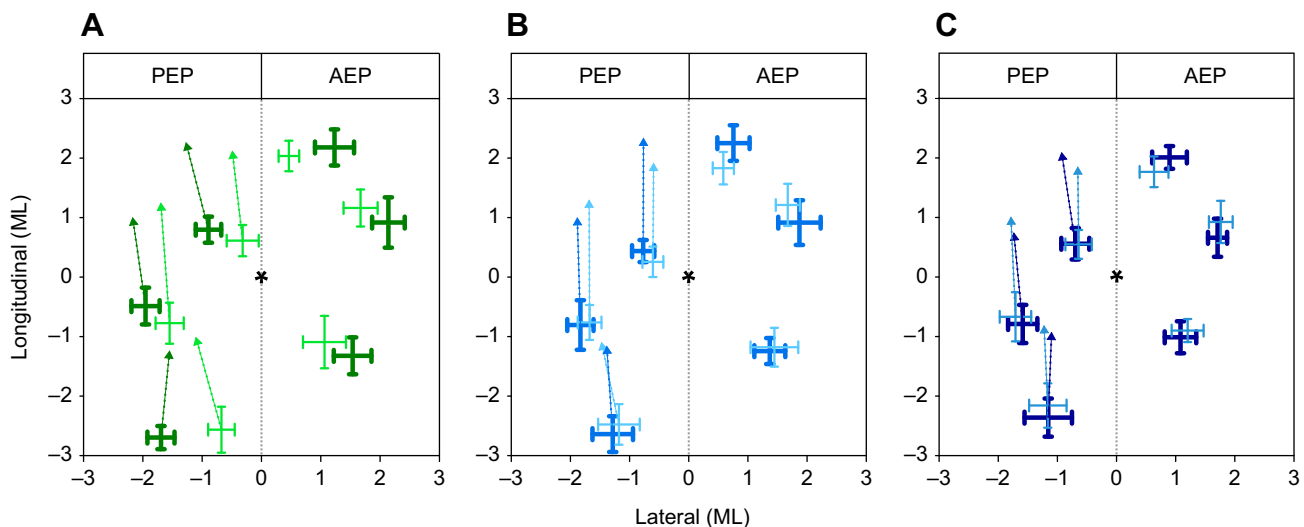

Fig. 4. Footfall geometry. (A) Average relative footfall positions of the legs of *C.a.* with respect to the petiole at the slowest (0–100 mm s^{-1}; dark green, bold) and fastest (300–400 mm s^{-1}, light green) walking speeds. (B) Average relative footfall positions of the legs of *C.b.*-I with respect to the petiole at the slowest (0–100 mm s^{-1}; blue, bold) and fastest (400–500 mm s^{-1}, light blue) walking speeds. (C) Average footfall positions of the legs of *C.b.*-III with respect to the petiole at the slowest (0–100 mm s^{-1}; dark blue, bold) and fastest (300–400 mm s^{-1}, blue) walking speeds. For each footfall position, six videos with three step cycles each were evaluated. Posterior extreme positions (PEP) are shown for the left body side and anterior extreme positions (AEP) for the right body side. For better comparison, leg movements are indicated on the left sides of the panels (PEP) as dotted arrows, with the arrowhead pointing at the AEP. x- and y-axes are normalized to body size (mesosoma length).
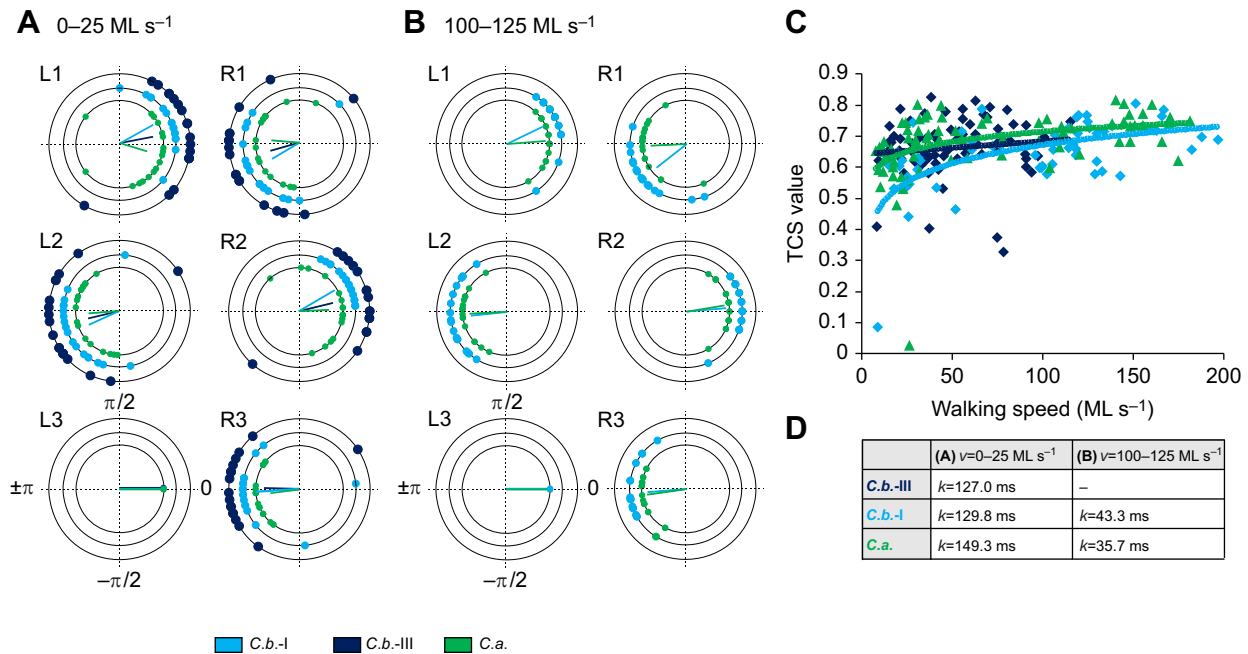
Fig. 5. Phase analysis. (A,B) Circular step cycle diagrams of the six legs analysed for *C.b.*-III (dark blue), *C.b.*-I (light blue) and *C.a.* (green) with respect to the left hind leg (L3). Phase plots of *C.b.*-III, *C.b.*-I and *C.a.* are shown in sequence from periphery to centre. Six videos with three step cycles each were analysed for different walking speed bins, (A) 0–25 ML s^{-1} and (B) 100–125 ML s^{-1}. Relative walking speeds above 100 ML s^{-1} were achieved by only a few *C.b.*-III ants; therefore, no phase plots were created. Each data point represents the onset of swing phase with respect to L3. The length of the mean phase vector (normalized to inner circle diameter) indicates the variance of the data points. (C) Tripod coordination strength (TCS), plotted as function of relative walking speed (*C.b.*-I: logarithmic regression: $y=0.09\ln x+0.27$, $R^2=0.37$; *C.b.*-III: linear regression: $y=0.0004x+0.64$, $R^2=0.01$; *C.a.*: logarithmic regression: $y=0.05\ln x+0.50$, $R^2=0.17$). (D) Data for phase plots of *C.b.*-I, *C.b.*-III and *C.a.* with circumference k, representing step cycle duration.

analysed with regard to absolute and relative walking speeds; that is, after normalization to body size.

Morphometric analysis

For morphometric analysis, mesosoma length and leg length were measured. *Cataglyphis bicolor* exhibited large variability in mesosoma length (2.39–4.96 mm), which was used as the main characteristic for sizing. In our sample, there were clearly more large than small individuals. Based on the morphometric data, ants of the species *C. bicolor* were divided into small (*C.b.*-I) and large ants (*C.b.*-III). *C.b.*-I ants were significantly smaller (mean±s.d. mesosoma length 2.96±0.33 mm, 2.39–3.46 mm) than *C.b.*-III ants (4.38±0.22 mm, 4.0–4.96 mm). *Cataglyphis albicans* (*C.a.*) was again smaller than *C.b.*–I (1.94±0.2 mm, 1.58–2.66 mm), although there were clear overlaps in values of mesosoma and leg lengths between the two species (Fig. 2).

Leg length was shortest in *C. albicans* and increased with body size in *C. bicolor* (Fig. 2). Front legs of *C.a.* were 32% shorter (3.5±0.35 mm) than those of *C.b.*-I (5.2±0.72 mm), on average, and front legs of *C.b.*-III (7.9±0.41 mm) were 34% longer than in *C.b.*-I. Middle legs of *C.a.* were 37% shorter (3.9±0.37 mm) than those of *C.b.*-I (6.2±0.87 mm), on average, and middle legs of *C.b.*-III (9.4±0.53 mm) were 34% longer than in *C.b.*-I. Hind legs averaged 5.4±0.49 mm in *C.a.* (35% shorter than in *C.b.*-I), 8.3±1.08 mm in *C.b.*-I and 12.4±0.66 mm in *C.b.*-III (33% longer than in *C.b.*-I).

In both species, the relationship between leg and mesosoma length was almost isometric (Tables S1 and S2). That is, larger ants have proportionally longer legs, and vice versa. The regression lines of the two species almost merge, which is why *C. albicans* may be considered a shrunk version of *C. bicolor* (Fig. 2) (see also Sommer and Wehner, 2012). The enlargement from the smallest *C. albicans*

to the largest *C. bicolor* is continuous in proportion, providing a natural size gradient. Along this size spectrum, the allometry of locomotion in *Cataglyphis* ants can be analysed by intraspecific and interspecific comparison.

Basic walking parameters

Walking parameters were analysed over the entire walking speed range in *C. bicolor* (*C.b.*-I: 29–516 mm s^{-1}, *C.b.*-III: 34–468 mm s^{-1}) and *C. albicans* (*C.a.*: 15–374 mm s^{-1}). We evaluated swing and stance phase duration, stride length, stride frequency and swing speed in relation to absolute and relative walking speed (mesosoma lengths per second, ML s^{-1}). Below, these walking parameters are compared between *C.b.*-I, *C.b.*-III and *C.a.* The results are presented in Table 1 and Fig. 3.

With regard to maximum walking speed, it is notable that *C. bicolor* ants reached higher absolute speeds than *C. albicans* individuals (Table 1). On a relative scale, however, small ants of *C. bicolor* and ants of *C. albicans* were clearly faster than large *C. bicolor* individuals. This is the reason why at high relative speeds only *C.b.*-I and *C.a.* may be compared meaningfully.

In both species, swing and stance phase durations shortened with increasing walking speed, with little difference between *C.b.*-I and *C.b.*-III and clear differences between the two species, *C. bicolor* and *C. albicans* (Table 1, Fig. 3A,B). Towards high walking speeds, swing phase duration levelled off with a power function nearing a value of 23 ms in *C.b.*-I and *C.b.*-III, and a minimum of 14 ms in *C.a.* Stance phase duration was as short as 7 ms in *C.a.*, while minimum stance phase duration in *C.b.*-I and *C.b.*-III was 9 and 11 ms, respectively.

With increasing walking speed, stride length increased. In comparison to *C. bicolor*, *C. albicans* showed clearly shorter

Fig. 6. Qualitative gait analysis. Podograms recorded in *C.b.*-III (A), *C.b.*-I (B) and *C.a.* (C) at slow (i), medium (ii) and high (iii) relative walking speeds, with corresponding colour indices plotted along the same time axes. Podograms illustrate the gait pattern of the six legs, with black bars indicating swing phases and white bars, stance phases (L: left leg; R: right leg; 1, 2 and 3: front, middle and hind leg). Each video frame was assigned an index number and a corresponding colour according to the leg coordination in that frame (see key). For an exact definition of gait patterns, see Fig. S3. To illustrate the differences in the time axes between slow, medium and high speed plots, corresponding time segments are indicated in grey between Ci and ii, and between Cii and iii, respectively.

stride lengths at the respective speeds (Table 1, Fig. 3C). Both species increased their limit of stride length, as determined by leg length, by the insertion of aerial phases. Aerial phases started to emerge at walking speeds around 300 mm s^{-1} in *C. bicolor* and at considerably slower speeds around 100 mm s^{-1} in *C. albicans* (compare gait analysis, Fig. 7; duty factor, Fig. S2).

Stride frequency increased with walking speed, with clear differences between *C. bicolor* and *C. albicans* (Table 1, Fig. 3D). *C.b.*-I reached higher absolute (and relative) walking

speeds than *C.b.*-III and, being smaller and having shorter legs, did so by higher stride frequency. Stride frequency of *C. bicolor* levelled off towards a value around 26 Hz beyond speeds of 300 mm s^{-1}. By comparison, no frequency plateau was observed in *C. albicans*. Here, stride frequency increased linearly up to almost 40 Hz (Fig. 3D).

Swing speed represents the velocity of leg movement during swing, and it increased almost linearly with walking speed. The fastest swing speeds of 0.86 m s^{-1} were reached only by *C.b.*-III,
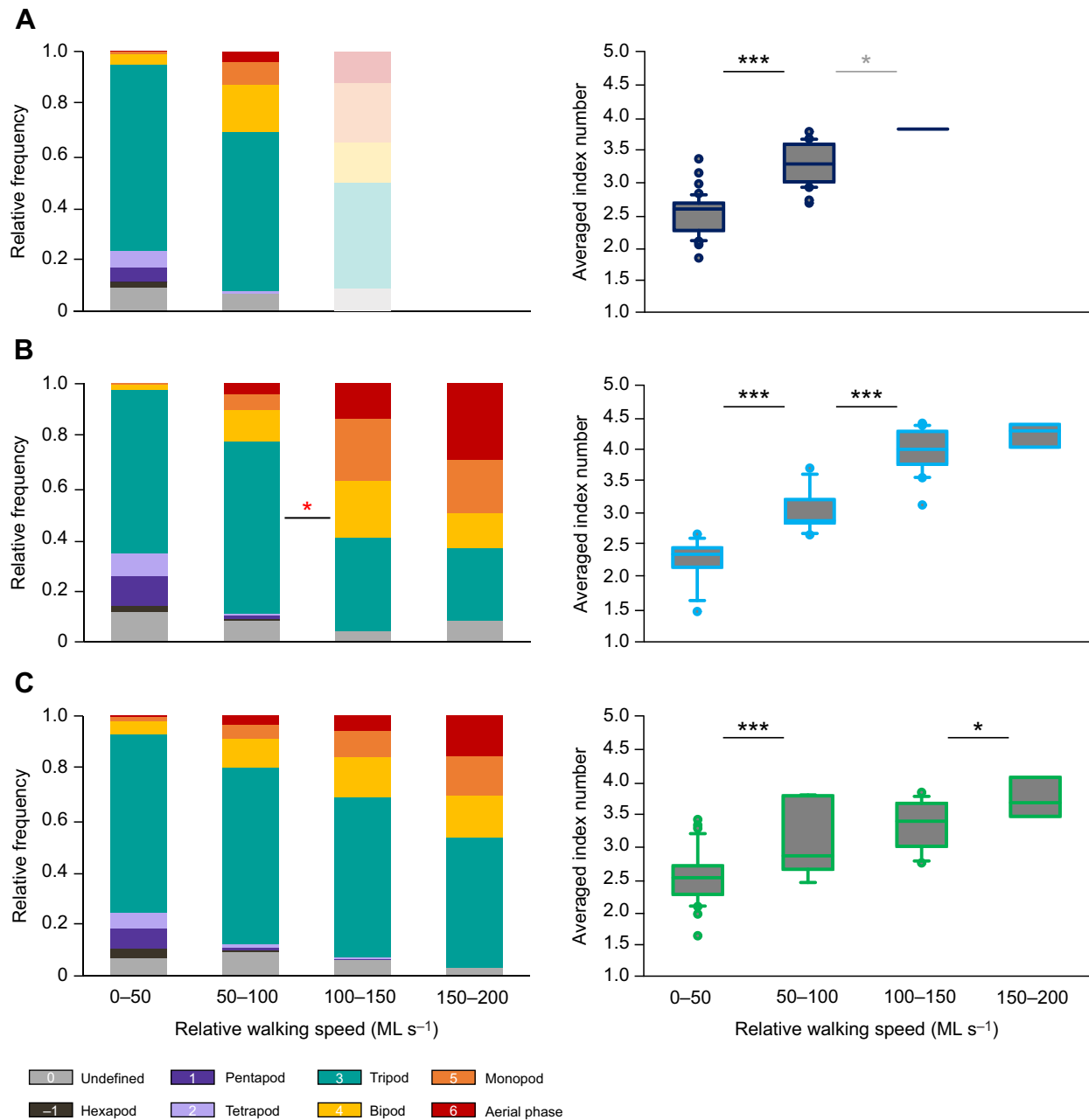
Fig. 7. Quantitative gait analysis. Quantitative gait analysis according to walking speed classes (0–50 to 150–200 ML s^{-1}) for *C.b.*-I (A, *n*=57), *C.b.*-III (B, *n*=75) and *C.a.* (C, *n*=60) ants. Data are shown as relative frequency plots (colour index, left) and averaged index number (number index, right) for the respective walking speed bins. Each video frame was assigned an index number and a corresponding colour according to the leg coordination in that frame (see key). For an exact definition of gait patterns see Fig. S3. No data were available for walking speeds >150 ML s^{-1} in *C.b.*-III and only *n*=2 ants of *C.b.*-III reached relative walking speeds of 100–150 ML s^{-1} (transparent, data not included in further comparisons, but illustrating trend). Notable differences in gait pattern distribution were observed in *C.b.*-I (B) between the 50–100 and 100–150 ML s^{-1} speed bins (asterisk, see also average index number). Statistically significant differences (one-way ANOVA) occurred between the 0–50 and 50–100 ML s^{-1} speed bins in all ant groups (***P<0.001), between the 50–100 and 100–150 ML s^{-1} speed bins only in *C. bicolor* (*C.b.*-III: *P<0.05, *C.b.*-I: ***P<0.001) and between the 100–150 and 150–200 ML s^{-1} speed bins only in *C.a.* (*P<0.05). When comparing the number indices of *C.b.*–I, *C.b.*-III and *C.a.* for the above speed bins, there were statistically significant differences only for the 100–150 ML s^{-1} bins (one-way ANOVA, ***P<0.001).

while *C.b.*-I and *C.a.* ants reached distinctly lower absolute swing speeds (Table 1). A typical characteristic of desert ant locomotion appeared in all *C. bicolor* and *C. albicans* ants: the middle legs performed the highest swing speeds. As a consequence, they spent less time in swing phase than did the front and hind legs (compare single leg pair analysis, Fig. S1; duty factor, Fig. S2).

An important part of this study was the analysis of walking parameters in relation to relative walking speed, and the striking

differences between *C.b.*-I and *C.a.* revealed by this approach at high walking speeds. Relative speeds above 100 ML s^{-1} were achieved by just a few large individuals of *C. bicolor*. This is why only *C.b.*-I and *C.a.* are compared in the higher speed classes. When looking at stance phase duration, no differences were discernible between *C.a.*, *C.b.*-I and *C.b.*-III (Fig. 3F). By comparison, clear differences were apparent in swing phase duration, stride length and stride frequency (Fig. 3E,G,H), with deviations appearing beyond

Table 1. Walking parameters of *Cataglyphis bicolor* and *Cataglyphis albicans*

Walking parameter	*C.b.*-I	*C.b.*-III	*C.a.*
Walking speed (mm s^{-1})	29.63–516.95	34.67–468.59	15.54–374.41
Walking speed (ML s^{-1})	8.72–196.60	8.27–115.46	7.79–181.37
Swing phase duration (ms)	22.59–62.56	22.69–95.67	13.77–118.89
Stance phase duration (ms)	9.35–162.12	10.93–169.43	7.31–215.50
Stride length (mm)	6.72–19.66	7.66–20.25	4.68–10.04
Stride length (ML)	1.98–7.30	1.83–4.81	2.35–5.31
Stride frequency (Hz)	4.43–29.39	3.67–25.16	2.97–39.01
Swing speed (mm s^{-1})	107.53–730.96	103.52–862.49	45.16–614.97
Swing speed (ML s^{-1})	31.64–267.41	24.70–198.63	22.63–293.19

C.b.-I, *Cataglyphis bicolor* small; *C.b.*-III, *Cataglyphis bicolor* large; *C.a.*, *Cataglyphis albicans*; ML, mesosoma length. Minimum and maximum values are shown.

walking speeds of 100 ML s^{-1}. Compared with *C.b.*-I, swing phase duration was noticeably shorter in *C.a.* beyond 100 ML s^{-1}, while stride frequency increased linearly beyond the maximum values recorded in *C.b.*-I (Fig. 3H). Relative stride length diverged clearly beyond 100 ML s^{-1}, with *C.b.*-I showing longer relative strides (Fig. 3G). When looking at relative swing speed, *C.a.* showed the highest values with 293 ML s^{-1}, followed by *C.b.*-I and *C.b.*-III (Table 1).

In summary, small intraspecific differences were observed for *C. bicolor* despite the clear size differences, while walking parameters differed considerably between *C. bicolor* and *C. albicans* (Fig. 3). *Cataglyphis bicolor* reached the highest walking speeds by means of stride lengths ranging up to 20 mm (7.3 ML), whereas *C. albicans* achieved high walking speeds by distinctly higher stride frequencies of up to 40 Hz. A clear deviation of locomotion patterns occurred between *C.b.*-I and *C.a.* beyond relative walking speeds of 100 ML s^{-1}, with differences concerning primarily the above parameters, swing phase duration, stride length and stride frequency.

Footfall geometry

Footfall patterns of the legs (tarsi) in the PEP (just before lift-off at end of stance) and in the AEP (just after touch-down at beginning of stance) were analysed in *C.a.*, *C.b.*-I and *C.b.*-III. Overall, *C.a.* showed relative footfall positions closer to the body, compared with *C.b.*-I and *C.b.*-III, in both AEPs and PEPs at medium and high walking speeds (Fig. 4). Unexpectedly, this relationship reversed at the slowest walking speeds (0–50 ML s^{-1}). Here, footfall positions were clearly more distant from the COM in *C.a.* In comparison, there were just small differences in footfall positions in *C.b.*-I and *C.b.*-III at the slowest and fastest walking speeds, respectively. In both species, the points of tarsal ground contact were relatively closer to the body at higher walking speeds.

Phase analysis

TCS provides a measure of tripod synchrony (e.g. Wosnitza et al., 2013). TCS values mostly ranged between 0.5 and 0.8 (with 1.0 indicating exact tripod synchrony), and increased towards higher walking speeds in both *C.a.* and *C.b.*-I. By contrast, TCS values were nearly constant over the entire speed range in *C.b.*-III. At the respective speeds, TCS values were higher in *C.b.*-III than in *C.b.*-I, and highest in *C.a.* (Fig. 5C).

These observations are reflected in the phase relationships of leg movements. Phase plots illustrate inter-leg coordination in circular diagrams (Fig. 5A,B), with the onset of the swing phase in the left hind leg (L3) taken as a reference. For all ants, a clear antiphase relationship between tripod groups L1, R2, L3 and R1, L2, R3 was evident, which agrees with TCS values provided above. This tripod coordination was observed over the entire walking speed range, although with small but consistent phase shifts between the legs within the step cycle.

It is striking that *C. albicans* exhibited clearly higher synchrony; that is, all three legs lifted off the ground and entered the swing phase almost simultaneously (phase shifts 0.01–0.03 or <1 ms at medium and high walking speeds), while at the slowest speeds the front legs tended to lift off first (Fig. 5A,B). At slow speeds, variance was highest and decreased with increasing walking speed.

In *C. bicolor*, by comparison, relative phase shifts occurred in the step cycle, which is consistent with the lower TCS values. Phase shifts were more pronounced in *C.b.*-I (phase shifts 0.06–0.08) than in *C.b.*-III (phase shifts around 0.03) (Fig. 5A,B). The hind legs were lifted off first, in both *C.b.*-I and *C.b.*-III individuals, followed by the middle and then the front legs. At the highest walking speeds, variance was lowest, and the synchrony of leg movements increased.

Duty factor is another parameter to describe phase relationships, primarily for a given leg pair. It characterizes the transition from walking to running, which occurs at values around 0.5 (strictly at 0.5 for bipedal locomotion; Alexander, 2003). In *C. bicolor*, with increasing speed, the hind legs were the first to fall below a duty factor of 0.5, followed by the front legs and finally the middle legs. Small individuals reached a duty factor value of 0.5 at slower absolute speeds (front legs: 181 mm s^{-1}, middle legs: 236 mm s^{-1}, hind legs: 124 mm s^{-1}) than large ants (front legs: 220 mm s^{-1}, middle legs: 276 mm s^{-1}, hind legs: 190 mm s^{-1}) (Fig. S2). As the middle legs were the last to drop to a duty factor below 0.5, they determined the threshold at which the transition from walking to running eventually occurred. In comparison, *C. albicans* entered this transition from walking to running at the slowest absolute walking speeds, with the hind and front legs simultaneously falling below a duty factor 0.5 at 118 mm s^{-1}, followed by the middle legs at 210 mm s^{-1} (Fig. S2).

When considering the duty factor in relation to relative walking speed, it is evident that the transition from walking to running is reversed between the two ant species in this perspective. Running commenced at slower relative speeds in *C. bicolor* (*C.b.*-I: 81 ML s^{-1}, *C.b.*-III: 63 ML s^{-1}) than in *C. albicans* (111 ML s^{-1}) (Fig. S2).

Gait analysis

Walking behaviour of *C. bicolor* and *C. albicans* was further characterized by a qualitative (podograms, Fig. 6) and quantitative gait analysis (Fig. 7). For a quantitative assessment, each frame of the high-speed videos was assigned an index number and a corresponding colour code that identifies the leg coordination in the respective frame. To quantify gait patterns over the observed speed range, the proportion of each pattern was determined by gait indexing for *C.b.*-I, *C.b.*-III and *C.a.* in adjacent speed bins. Data were compared regarding both absolute (Fig. S4) and relative speed (Fig. 7), although our main focus was on relative data.

In gait analysis focused on relative walking speed, walking patterns differed significantly between *C. bicolor* (*C.b.*-I) and *C. albicans* beyond speeds of about 100 ML s^{-1} (Fig. 7). Notably, there was a distinct change in gait pattern in *C.b.*-I around 100 ML s^{-1} (while *C.b.*-III very rarely reached that speed). Below

100 ML s^{-1}, tripod gait dominated in all ant groups with well above 60% of the video frames. Above 100 ML s^{-1}, tripod fraction was replaced partially by bipod, monopod and aerial situations, which means that movements of the legs in the tripods sped up and tripod swing phases started to overlap. This replacement was gradual in *C. albicans* (tripod percentages 69%, 68%, 61% and 50% at 0–50, 50–100, 100–150 and 150–200 ML s^{-1}, respectively), while in *C. bicolor* (*C.b.*-I) an abrupt drop occurred from 66% tripod frames in the 50–100 ML s^{-1} bin to 36% in the 100–150 ML s^{-1} bin (asterisk in Fig. 7B) (0–50 ML s^{-1}: 63%, 150–200 ML s^{-1}: 28%). Thus, *C. albicans* showed a generally high tripod proportion over the entire walking speed range, while *C. bicolor* changed to an aerial phase pattern above 100 ML s^{-1}. Notable fractions of hexapod, pentapod and tetrapod support occurred only in the 0–50 ML s^{-1} speed bin, together amounting to some 18% across all ant groups.

Regarding mean index numbers, statistically significant differences occurred between *C. bicolor* and *C. albicans* when analysing walking speed class 100–150 ML s^{-1} (one-way ANOVA, Holm–Šidák method: $P<0.001$), confirming differences in locomotion pattern beyond about 100 ML s^{-1}. Statistically significant differences between neighbouring speed bins occurred at slow walking speeds (between 0–50 and 50–100 ML s^{-1}) for all ant groups ($P<0.001$), at faster walking speeds (between 50–100 and 100–150 ML s^{-1}) only for *C. bicolor* ($P<0.001$) and at the fastest speeds (between 100–150 and 150–200 ML s^{-1}) only for *C. albicans* ($P<0.05$), as indicated by the results of one-way ANOVA (Fig. 7).

In summary, the consistently high fraction of tripod coordination in *C. albicans* and the comparatively small incorporation of aerial phases are notable. Statistically significant differences in the index distribution between *C. bicolor* and *C. albicans* at relative walking speeds above 100 ML s^{-1} further underscore the use of different locomotor strategies in the transition from medium to high walking speeds ('trotting to galloping' when using terms from quadruped locomotion). In this context, the clear change in gait pattern in *C.b.*-I between <100 and >100 ML s^{-1} is remarkable. By comparison, rather small differences occur among differently sized individuals of *C. bicolor*.

DISCUSSION
The desert ant species *C. albicans* and *C. bicolor* occupy similar ecological niches, and the two species are observed in the same habitats, including parts of desert-like steppes in Tunisia (Wehner, 1983). Despite ecological similarities, the species differ in body size, covering a broad spectrum from 1.6 to 5.0 mm mesosoma length (Sommer and Wehner, 2012). Interestingly, the morphometric data of the largest individuals of *C. albicans* overlap with those of the smallest *C. bicolor* individuals, and leg and mesosoma lengths show similar size dependencies across the two species. Therefore, *C. albicans* may be regarded a miniaturized isometric transformation of *C. bicolor*. Based on this almost isometric relationship, one might assume that *C.b.*-I, *C.b.*-III and *C.a.* either use the same locomotor strategies, or that size-related differences in walking behaviour occur between all three groups. Instead, we found only small differences in the locomotion performance between *C.b.*-I and *C.b.*-III, while *C. albicans* exhibited a clearly different walking behaviour.

Maximum absolute and relative walking speeds
One might expect that larger ants would be able to achieve higher walking speeds. Surprisingly, small *C. bicolor* ants reached the highest speeds, irrespective of whether these were determined in absolute or relative terms (maximum speed: 516 mm s^{-1} or 196 ML s^{-1}). By contrast, larger individuals of this species reached considerably lower maximum speeds (468 mm s^{-1} or 115 ML s^{-1}). As expected, the smallest-sized species of our study, *C. albicans* (maximum speed: 374 mm s^{-1} or 181 ML s^{-1}), was unable to keep up with *C. bicolor* on an absolute scale, although these ants were able to outcompete the up to 3 times larger representatives of *C.b.*-III on a relative scale. Converted to body lengths per second, these maximum speeds correspond to 70 BL s^{-1} (*C.a.*), 80 BL s^{-1} (*C.b.*-I) and 49 BL s^{-1} (*C.b.*-III), respectively. Significantly higher relative walking speeds are achieved by only few arthropod species, such as *Cataglyphis bombycina* (108 BL s^{-1}), *Cicindela eburneola* (171 BL s^{-1}) or *Paratarsotomus macropalpis* (up to 377 BL s^{-1}) (Pfeffer et al., 2019; Kamoun and Hogenhout, 1996; Rubin et al., 2016).

The variation in maximum absolute walking speeds within the *C. bicolor* species illustrates clearly that scaling of walking speed depends on body size, or body mass, as the largest animals are not the fastest (Hirt et al., 2017). In this context, different studies have suggested that speed scaling depends on body mass range (Iriarte-Díaz, 2002; Hurlbert et al., 2008; Fuentes, 2016). Other studies investigated the influence of morphology, locomotion energetics and biomechanics (Garland, 1983; Bejan and Marden, 2006; Iriarte-Díaz, 2002; Dick and Clemente, 2017). The authors concluded that the walking speed of running animals is limited by the capacity of their muscles and bones to withstand the stress of touch-down forces (Biewener, 1982; Clemente et al., 2012; Hirt et al., 2017) and that there is a limit where larger body size inevitably reduces maximum speed (Dick and Clemente, 2017). Maximum absolute walking speed of small ant species such as *C. fortis* (~600 mm s^{-1}, ML: ~2.8 mm) and the even smaller *C. bombycina* (~800 mm s^{-1}, ML: ~2.5 mm) may fit into this line of argument (Pfeffer et al., 2019). Contrary to this reasoning, however, *C. albicans* is the smallest *Cataglyphis* species studied to date (see also Sommer and Wehner, 2012) but does not reach the highest (absolute or relative) walking speeds compared with small *C. bicolor* (*C.b.*-I) individuals. Smaller individuals may have different scaling slopes from larger individuals or species (Hurlbert et al., 2008). Apparently, there is a limit where even the smallest animals cannot increase walking speed further (Hirt et al., 2017). Leg length is obviously restricted by body size, within limits, and further by the inertial momentum inherent to long legs. Stride frequency cannot compensate for very short leg lengths as it is limited by the contraction and relaxation kinetics of leg muscle, and further by the viscosity of the involved media (Rubin et al., 2016). This appears to be demonstrated by stride frequency plateaus observed in many small animals (see also Wahl et al., 2015) (compare Fig. 3D,H).

Size-dependent strategies for reaching high walking speeds
Here, we report that differently sized ants use somewhat different locomotion strategies to achieve high speeds. The smallest ants, *C. albicans*, employ extremely high stride frequencies and incorporate aerial phases to reach high walking speeds, while the largest individuals of *C. bicolor* rely more on an increase in stride length. These large individuals are unable to sustain aerial phases to any appreciable extent, unlike their smaller kin and the small *C. albicans*. Body size and correspondingly longer legs and associated inertial momentum appear to be the reasons here. Small *C. bicolor* individuals – in the context of this study the medium-sized ants – can employ both high stride frequencies and aerial phases, while maintaining the gait pattern of their large conspecifics, resulting in the highest walking speeds. Ultimately,

both stride length and stride frequency contribute to high walking speeds and typically increase in close accord (Full and Tu, 1991; Bender et al., 2011; Reinhardt and Blickhan, 2014), at least within a given gait. This is part of the optimization of spatial and temporal movement parameters to reach high walking speeds (Heglund et al., 1974; Heglund and Taylor, 1988).

It is not surprising that, within *C. bicolor*, *C.b.*-III shows longer stride lengths at the same absolute speeds compared with *C.b.*-I. This can be attributed to their longer legs (Fig. 2). Rather, it is surprising that the two extreme size classes in *C. bicolor* exhibit quite similar maximum stride lengths, *C.b.*-I with 19.7 mm and *C.b.*-III with 20.2 mm, despite their notable, up to 2-fold, difference in body length, averaging 2.96 and 4.98 mm mesosoma length, respectively. The incorporation of aerial phases is responsible for this, as they can significantly increase stride length. In comparison, the small *C. albicans* have very short stride lengths with maximum values of 10 mm, in combination with the incorporation of aerial phases at relatively slow speeds (below 100 mm s^{-1}). Altogether, there is just a doubling of stride length in *C. albicans*, while *C. bicolor* almost triples this walking parameter. Accordingly, *C. albicans* increases walking speed only to a small extent via stride length.

Instead, *C. albicans* employs primarily very high stride frequencies of up to 40 Hz to increase walking speed. The American cockroach, *Periplaneta americana*, by comparison, reaches frequencies of about 27 Hz at walking speeds up to 1.5 m s^{-1} (Full and Tu, 1991), and the fastest desert ant *C. bombycina* reaches up to 47 Hz at 0.85 m s^{-1} (Pfeffer et al., 2019). The highest reported stride frequency of 135 Hz is achieved by the small mite *P. macropalpis* (Rubin et al., 2016). A typical stride frequency limitation towards the highest walking speeds could be observed in *C. bicolor*, with maximum frequency slightly lower in the larger *C.b.*-III ants. The lower maximum stride frequency of *C.b.*-III appears to be related to their larger stride length, afforded by larger body size, leg length and resulting leg inertial momentum. This effect has been demonstrated in both arthropods and mammals, which differ significantly in size (Heglund et al., 1974; Heglund and Taylor, 1988), and it is further illustrated by clear interspecific differences in swing and stance phase durations (Table 1, Fig. 3).

Size- and species-specific leg synchrony and footprint clustering

Concerning static and dynamic locomotion, phase relationships and footprint positions are informative parameters (Ting et al., 1994). At lower walking speeds, walking performance of ants is characterized by stride lengths below maximum span, and at higher speeds by gaps between successive tripods, indicating a temporary loss of static equilibrium and aerial phases (Zollikofer, 1994b) (Fig. 1). This is reflected in footprint positions of *C. albicans* and *C. bicolor*, with a general tendency for all ants to have relative footprint positions closer to the body with increasing walking speeds (Fig. 4). The most striking differences between low and high speeds were observed in footprint positions of *C. albicans*, indicating considerable differences between statically stable walking at low speeds and dynamically stable walking at high speeds (Ting et al., 1994; Zollikofer, 1994c; Spagna et al., 2011). Legs placed in sprawled positions around the body can provide a stable posture for resistance against wind or other disturbances (Alexander, 1971) and this offers static stability for insects during locomotion at the lowest speeds (Ting et al., 1994). At higher walking speeds, this quasi-static model is considered insufficient

and running appears better modelled by a 'spring-loaded inverted pendulum' approach (SLIP; Alexander, 1988, 2003; Holmes et al., 2006; Spagna et al., 2011). Accordingly, footprint positions indicate statically stable walking at the lowest walking speeds and dynamic stability at higher speeds. The clear difference between footprint positions at low and high speeds in *C. albicans* might be related to their short legs and support stable walking in this small species, while all *C. bicolor* ants show more dynamic walking over the entire speed range.

When considering phase relationships, the high synchrony of the leg pairs in *C. albicans* is striking, while in *C. bicolor* the clear tendency was observed for the front legs to lift off last (Fig. 5). This is also reflected in the slightly higher TCS value and the generally higher tripod fraction of *C. albicans*. TCS increases with higher walking speeds in both species, leading to an increase in tripod coordination accuracy (Wahl et al., 2015; Pfeffer et al., 2019). As mentioned above, in animals walking on more than one leg pair, phase shifts can avoid aerial phases for the whole animal up to a certain point (Hildebrand, 1985). The tendency for the front legs to lift off last in *C. bicolor* ants would appear to be related to the late incorporation of aerial phases with increasing absolute velocities, compared with *C. albicans*.

Gait continuum and relative speed

In insects, different walking patterns have been observed and defined, these patterns merging into each other smoothly in a velocity-dependent continuum (Fig. 6) (Hughes, 1952; Wilson, 1966; Schilling et al., 2013; Dürr et al., 2018; Pfeffer et al., 2019). While tripod coordination is described as a major walking pattern (e.g. Zollikofer, 1994a), insect gaits are considered variable rather than fixed patterns (Grabowska et al., 2012; Wosnitza et al., 2013; Wahl et al., 2015; Isakov et al., 2016). Many fast-running insects, such as ants, beetles and cockroaches, also use combinations with fewer than three legs in stance to achieve high walking speeds (Hughes, 1952; Zollikofer, 1994a,b,c; Bender et al., 2011). Further, the inclusion of aerial phases has been described, for example, in cockroaches (Full and Tu, 1990, 1991); initial analyses were in vertebrates (Heglund et al., 1974). Nonetheless, the transition between insect walking patterns is not yet fully understood (Graham, 1985; Mendes et al., 2013), although possible solutions can be given using neural networks (Schilling and Cruse, 2020). In the present study, the description of gait patterns is used to provide a quantitative locomotion analysis. In conjunction with the description of other walking parameters and phase analyses, size- and velocity-dependent differences in locomotor performance can be inferred.

Most intriguingly, our gait analysis indicates clear differences in walking behaviour between *C. albicans* and the similarly sized (small) *C. bicolor* individuals (*C.b.*-I). In *C. albicans*, a consistent dominance of the tripod gait was observed, and gait patterns merged into each other smoothly with increasing (relative) speed. By contrast, a significant change in gait pattern was observed in *C. bicolor*, occurring around 100 ML s^{-1} (Fig. 7). Transitions at relative speeds of about 100 ML s^{-1} were noticed in several walking parameters, gait patterns and phase analyses during our study, and they appear to indicate a gait change in the small *C. bicolor* ants (compare Heglund et al., 1974). As described previously for *C. fortis* (Wahl et al., 2015), incorporation of aerial phases into the gait pattern occurs as stride frequency levels off, allowing further speed increases by extending stride length beyond the morphological limit of leg span. Thus, a saturation of stride frequency with increasing speed could be an indicator of a gait

change (Heglund et al., 1974). Indeed, at 100 ML s^{-1} in *C.b.*-I ants, four events coincide: (i) a frequency plateau is approached (Fig. 3D,H), (ii) aerial phases start to be included (Fig. 7B; Fig. S4B), (iii) fractions of gait patterns change significantly (Fig. 7B; Fig. S4B) and (iv) duty factor decreases below 0.5 (Fig. S2). As only two of the large *C. bicolor* individuals had just about exceeded 100 ML s^{-1}, no statement can be made for *C.b.*-III.

Regarding gait patterns, previous studies on insects did not describe gait changes comparable to those observed in quadrupeds or bipeds (Schilling et al., 2013; Dürr et al., 2018). Nevertheless, our data indicate that, in small *C. bicolor* ants, there occurs a rather abrupt gait change despite a basic gait continuum (Figs 6 and 7). This is signified by the coincident changes in key walking parameters; namely, plateauing stride frequency, the appearance of aerial phases, a decrease in the percentage of tripod coordination and a drop of duty factor below 0.5. We tentatively applied calculations regarding gait changes in quadrupeds (Heglund et al., 1974) to the two desert ant species studied here. According to the formulas of Heglund and co-workers (1974), a gait change in the desert ants would be expected at stride frequencies around 20 Hz, stride lengths slightly below 5 mm and walking speeds just below 100 mm s^{-1}. Quite unexpectedly, stride frequency values deviate only slightly and stride length and speed deviate by not more than a factor of 3 from where the assumed gait change occurs in *C. bicolor* (see Fig. 3). This is intriguing as the formulas presented by Heglund and co-workers (1974) were derived for large mammals such as horses where leg inertia plays a significant role (see SLIP approach noted above; Alexander, 1988, 2003; Holmes et al., 2006; Spagna et al., 2011). Walking in small insects, by contrast, would be expected to be determined more by viscous and elastic forces.

In comparison to *C. bicolor*, no sudden changes in the fractions of gait patterns occurred in *C. albicans*, or in stride frequency saturation, and nor did all three leg pairs fall below duty factor 0.5 consistently at the highest walking speeds. Intriguingly, stride frequency increased almost linearly with speed in *C.a.* up to almost 40 Hz. The assumption that aerial phases occur when a frequency plateau is reached thus does not apply to *C.a.* Indeed, aerial phases occur at speeds below 100 mm s^{-1}/50 ML s^{-1} in this ant species. Small body size and accordingly short legs would hence appear to be decisive for *C. albicans* to achieve high stride frequencies. This is consistent with the statement that small animals generally reach higher stride frequencies and change their walking patterns at comparatively lower walking speeds (Blickhan and Full, 1993; Pfeffer et al., 2019). Smaller animals' stride frequencies might be limited by other factors from those of large animals, explaining the missing frequency plateau of *C.a.* and the extremely high frequency of the mite *P. macropalpis* (Rubin et al., 2016). The relative importance of viscous and elastic versus inertial forces may again play a role here.

Conclusion

In summary, it is evident that *C. bicolor* individuals use the same locomotor strategy across all body sizes, with small ants reaching the highest walking speeds by increasing their stride length through incorporation of aerial phases. Small differences in walking parameters between *C.b.*-I and *C.b.*-III appear to be due to the fact that large ants do not reach the highest walking speeds. *Cataglyphis albicans*, by contrast, reach high walking speeds by high stride frequencies ranging up to 40 Hz and the incorporation of aerial phases at low speeds, concomitant with a high synchrony of leg movements. Most intriguingly, the two closely related desert ant species, *C. bicolor* and *C. albicans*, exhibiting almost isometric

proportions concerning mesosoma and leg lengths, show distinct differences in walking behaviour. From this perspective, it was surprising that all ants tended to show the same overall strategy at low walking speeds, and significant differences occurred only at higher speeds, with *C. bicolor* exhibiting a gait change around 100 ML s^{-1}.

It remains as yet unresolved to what extent body size has an influence on these differences in locomotion. We cannot ascertain which differences in the three ant groups were size specific and which were species specific. The fact that *C.b.*-I and *C.b.*-III show only small differences in walking behaviour would appear to argue for species-specific consistency, as do the distinct differences to *C.a.*, despite the notable overlap in body size with *C.b.*-I. Further analyses of walking behaviour in terms of relative speed would help to determine the exact influence of body size and promote comparison of locomotor patterns within and between species.

References

Agosti, D. (1990). Review and reclassification of *Cataglyphis* (*Hymenoptera, Formicidae*). *J. Nat. Hist.* **24**, 1457-1505. doi:10.1080/00222939000770851

Alexander, R. M. (1971). *Size and Shape (No. 29)*. Hodder Education.

Alexander, R. M. (1988). *Elastic Mechanism in Animal Movement*. Cambridge University Press.

Alexander, R. M. (2003). *Principles of Animal Locomotion*. Princeton University Press.

Andersen, A. N., Hoffmann, B. D. and Oberprieler, S. K. (2020). Megadiversity in the Ant Genus *Melophorus*: The *M. rufoniger* Heterick, Castalanelli and Shattuck species group in the top end of Australia's Northern Territory. *Diversity*, **12**, 386. doi:10.3390/d12100386

Ayali, A., Borgmann, A., Büschges, A., Couzin-Fuchs, E., Daun-Gruhn, S. and Holmes, P. (2015). The comparative investigation of the stick insect and cockroach models in the study of insect locomotion. *Current Opinion in Insect Science* **12**, 1-10. doi:10.1016/j.cois.2015.07.004

Bejan, A. and Marden, J. H. (2006). Unifying constructal theory for scale effects in running, swimming and flying. *J. Exp. Biol.* **209**, 238-248. doi:10.1242/jeb.01974

Bender, J. A., Simpson, E. M., Tietz, B. R., Daltorio, K. A., Quinn, R. D. and Ritzmann, R. E. (2011). Kinematic and behavioral evidence for a distinction between trotting and ambling gaits in the cockroach *Blaberus discoidalis*. *J. Exp. Biol.* **214**, 2057-2064. doi:10.1242/jeb.056481

Berens, P. (2009). CircStat: a MATLAB toolbox for circular statistics. *J. Stat. Softw.* **31**, 1-21. doi:10.18637/jss.v031.i10

Biewener, A. A. (1982). Bone strength in small mammals and bipedal birds: do safety factors change with body size? *J. Exp. Biol.* **98**, 289-301. doi:10.1242/jeb.98.1.289

Blickhan, R. and Full, R. J. (1993). Similarity in multilegged locomotion: bouncing like a monopode. *J. Comp. Physiol. A* **173**, 509-517. doi:10.1007/BF00197760

Burd, M. (2000). Body size effects on locomotion and load carriage in the highly polymorphic leaf-cutting ants *Atta colombica* and *Atta cephalotes*. *Behav. Ecol.* **11**, 125-131. doi:10.1093/beheco/11.2.125

Clemente, C. J., Withers, P. C. and Thompson, G. (2012). Optimal body size with respect to maximal speed for the yellow-spotted monitor lizard (*Varanus panoptes*; *Varanidae*). *Physiol. Biochem. Zool.* **85**, 265-273. doi:10.1086/665275

Clifton, G. T., Holway, D. and Gravish, N. (2020). Uneven substrates constrain walking speed in ants through modulation of stride frequency more than stride length. *R. Soc. open sci.* **7**, 192068. doi:10.1098/rsos.192068

Dick, T. J. and Clemente, C. J. (2017). Where have all the giants gone? How animals deal with the problem of size. *PLoS Biol.* **15**, e2000473. doi:10.1371/journal.pbio.2000473

Dürr, V., Theunissen, L. M., Dallmann, C. J., Hoinville, T. and Schmitz, J. (2018). Motor flexibility in insects: adaptive coordination of limbs in locomotion and near-range exploration. *Behav. Ecol. Sociobiol.* **72**, 1-21. doi:10.1007/s00265-017-2412-3

Fabricius, J. C. (1793). *Entomologia systematica emendate et aucta secundum classes, ordines, genera, species ajectis synonymis, locis, observationibus, descriptionibus*. C. G. Proft, Hafniae.

Fuentes, M. A. (2016). Theoretical considerations on maximum running speeds for large and small animals. *J. theor. Biol.* **390**, 127-135. doi:10.1016/j.jtbi.2015.10.039

Full, R. J. and Tu, M. S. (1990). Mechanics of six-legged runners. *J. Exp. Biol.* **148**, 129-146. doi:10.1242/jeb.148.1.129

Full, R. J. and Tu, M. S. (1991). Mechanics of a rapid running insect: two-, four- and six-legged locomotion. *J. Exp. Biol.* **156**, 215-231. doi:10.1242/jeb.156.1.215

Garland, T., Jr (1983). Scaling the ecological cost of transport to body mass in terrestrial mammals. *Am. Nat.* **121**, 571-587. doi:10.1086/284084

Gehring, W. J. and Wehner, R. (1995). Heat shock protein synthesis and thermotolerance in *Cataglyphis*, an ant from the Sahara desert. *Proc. Natl. Acad. Sci. USA* **92**, 2994-2998. doi:10.1073/pnas.92.7.2994

Grabowska, M., Godlewska, E., Schmidt, J. and Daun-Gruhn, S. (2012). Quadrupedal gaits in hexapod animals–inter-leg coordination in free-walking adult stick insects. *J. Exp. Biol.* **215**, 4255-4266. doi:10.1242/jeb.073643

Graham, D. (1985). Pattern and control of walking in insects. *Adv. Insect. Physiol.* **18**, 31-140. doi:10.1016/S0065-2806(08)60039-9

Heglund, N. C. and Taylor, C. R. (1988). Speed, stride frequency and energy cost per stride: how do they change with body size and gait? *J. Exp. Biol.* **138**, 301-318. doi:10.1242/jeb.138.1.301

Heglund, N. C., Taylor, C. R. and McMahon, T. A. (1974). Scaling stride frequency and gait to animal size: mice to horses. *Science* **186**, 1112-1113. doi:10.1126/science.186.4169.1112

Hildebrand, D. M. (1985). Walking and running. In *Functional Vertebrate Morphology* (ed. M. Hildebrand, D.M. Bramble, K.F. Liem and D.B. Wake), pp. 38-57. Belknap Press of Harvard University Press.

Hirt, M. R., Jetz, W., Rall, B. C. and Brose, U. (2017). A general scaling law reveals why the largest animals are not the fastest. *Nat. Ecol. Evol.* **1**, 1116-1122. doi:10.1038/s41559-017-0241-4

Holmes, P., Full, R. J., Koditschek, D. and Guckenheimer, J. (2006). The dynamics of legged locomotion: Models, analyses, and challenges. *SIAM Rev.* **48**, 207-304. doi:10.1137/S0036144504445133

Hughes, G. M. (1952). The Co-Ordination of insect movements: I The walking movements of insects. *J. Exp. Biol.* **29**, 267-285. doi:10.1242/jeb.29.2.267

Humeau, A., Piñeirua, M., Crassous, J. and Casas, J. (2019). Locomotion of ants walking up slippery slopes of granular materials. *Integr. Organismal Biol.* **1**, obz020. doi:10.1093/iob/obz020

Hurlbert, A. H., Ballantyne, F. and Powell, S. (2008). Shaking a leg and hot to trot: the effects of body size and temperature on running speed in ants. *Ecol. Entomol.* **33**, 144-154. doi:10.1111/j.1365-2311.2007.00962.x

Iriarte-Díaz, J. (2002). Differential scaling of locomotor performance in small and large terrestrial mammals. *J. Exp. Biol.* **205**, 2897-2908. doi:10.1242/jeb.205.18.2897

Isakov, A., Buchanan, S. M., Sullivan, B., Ramachandran, A., Chapman, J. K., Lu, E. S. and … de Bivort, B. (2016). Recovery of locomotion after injury in *Drosophila melanogaster* depends on proprioception. *J. Exp. Biol.* **219**, 1760-1771. doi:10.1242/jeb.133652

Kamoun, S. and Hogenhout, S. A. (1996). Flightlessness and rapid terrestrial locomotion in tiger beetles of the *Cicindela L.* subgenus *Rivacindela* van Nidek

from saline habitats of Australia (*Coleoptera: Cicindelidae*). *Coleopt.Bull.* **50**, 221-230.

Mendes, C. S., Bartos, I., Akay, T., Márka, S. and Mann, R. S. (2013). Quantification of gait parameters in freely walking wild type and sensory deprived *Drosophila melanogaster*. *eLife* **2**, e00231. doi:10.7554/eLife.00231.001

Pfeffer, S. E., Wahl, V. L. and Wittlinger, M. (2016). How to find home backwards? Locomotion and inter-leg coordination during rearward walking of *Cataglyphis fortis* desert ants. *J. Exp. Biol.* **219**, 2110-2118. doi:10.1242/jeb.137778

Pfeffer, S. E., Wahl, V. L., Wittlinger, M. and Wolf, H. (2019). High-speed locomotion in the Saharan silver ant, *Cataglyphis bombycina*. *J. Exp. Biol.* **222**, jeb198705. doi:10.1242/jeb.198705

Prenter, J., Pérez–Staples, D. and Taylor, P. W. (2010). The effects of morphology and substrate diameter on climbing and locomotor performance in male spiders. *Func. Ecol.* **24**, 400-408. doi:10.1111/j.1365-2435.2009.01633.x

Prenter, J., Fanson, B. G. and Taylor, P. W. (2012). Whole-organism performance and repeatability of locomotion on inclines in spiders. *Animal Behav.* **83**, 1195-1201. doi:10.1016/j.anbehav.2012.02.010

Reinhardt, L. and Blickhan, R. (2014). Level locomotion in wood ants: evidence for grounded running. *J. Exp. Biol.* **217**, 2358-2370.

Roger, J. (1859). Beiträge zur Kenntnis der Ameisenfauna der Mittelmeerländer. *Erstes Stück. – Berliner ent. Z.* **3**, 225-259. doi:10.1002/mmnd.18590030209

Rubin, S., Young, M. H. Y., Wright, J. C., Whitaker, D. L. and Ahn, A. N. (2016). Exceptional running and turning performance in a mite. *J. Exp. Biol.* **219**, 676-685. doi:10.1242/jeb.128652

Schilling, M. and Cruse, H. (2020). Decentralized control of insect walking: a simple neural network explains a wide range of behavioral and neurophysiological results. *PLoS Comp. Biol.* **16**, e1007804. doi:10.1371/journal.pcbi.1007804

Schilling, M., Hoinville, T., Schmitz, J. and Cruse, H. (2013). Walknet, a bio-inspired controller for hexapod walking. *Biol. Cybern.,* **107**, 397-419. doi:10.1007/s00422-013-0563-5

Seidl, T. and Wehner, R. (2008). Walking on inclines: how do desert ants monitor slope and step length. *Front. Zool.* **5**, 1-15. doi:10.1186/1742-9994-5-8

Sommer, S. and Wehner, R. (2012). Leg allometry in ants: extreme long-leggedness in thermophilic species. *Arthropod Struct. Dev.* **41**, 71-77. doi:10.1016/j.asd.2011.08.002

Spagna, J. C., Valdivia, E. A. and Mohan, V. (2011). Gait characteristics of two fast-running spider species (*Hololena adnexa* and *Hololena curta*), including an aerial phase (*Araneae: Agelenidae*). *J. Arachnol.* **39**, 84-91. doi:10.1636/B10-45.1

Ting, L. H., Blickhan, R. and Full, R. J. (1994). Dynamic and static stability in hexapedal runners. *J. Exp. Biol.* **197**, 251-269. doi:10.1242/jeb.197.1.251

Wahl, V., Pfeffer, S. E. and Wittlinger, M. (2015). Walking and running in the desert ant *Cataglyphis fortis*. *J. Comp. Physiol. A,* **201**, 645-656. doi:10.1007/s00359-015-0999-2

Wehner, R. (1983). Taxonomie, Funktionsmorphologie und Zoogeographie der saharischen Wüstenameise *Cataglyphis fortis* (Forel 1902) stat. nov. *Senckenbergiana Biol.* **64**, 89-132.

Wehner, R. and Wehner, S. (2011). Parallel evolution of thermophilia: daily and seasonal foraging patterns of heat–adapted desert ants: *Cataglyphis* and *Ocymyrmex* species. *Physiol. Entom.* **36**, 271-281. doi:10.1111/j.1365-3032.2011.00795.x

Wilson, D. M. (1966). Insect walking. *Annu. Rev. Entomol.* **11**, 103-122. doi:10.1146/annurev.en.11.010166.000535

Wosnitza, A., Bockemühl, T., Dübbert, M., Scholz, H. and Büschges, A. (2013). Inter-leg coordination in the control of walking speed in *Drosophila*. . *J. Exp. Biol.* **216**, 480-491. doi:10.1242/jeb.078139

Yeoh, C. E. and Yi, H. (2021). Conceptual Design of the Combinable Legged Robot Bio-Inspired by Ants' Structure. *Appl. Sci.* **11**, 1379. doi:10.3390/app11041379

Zollikofer, C. (1994a). I. Stepping patterns in ants-influence of speed and curvature. *J. Exp. Biol.* **192**, 95-106.

Zollikofer, C. (1994b). II: Stepping patterns in ants-influence of body morphology. *J. Exp. Biol.* **192**, 107-118. doi:10.1242/jeb.192.1.107

Zollikofer, C. (1994c). III. Stepping patterns in ants-influence of load. *J. Exp. Biol.* **192**, 119-127. doi:10.1242/jeb.192.1.119